Dynamics and Stability of Acoustic Wavefronts in the Ocean

Oleg A. Godin
CIRES/Univ. of Colorado and NOAA/Earth System Research Lab.
Physical Sciences Division, R/PSD99
325 Broadway
Boulder, CO 80305-3328
phone: (303) 497-6558   fax: (303) 497-5862   email: oleg.godin@noaa.gov

LONG-TERM GOALS

- To develop a method of modeling sound propagation in an environment with multi-scale inhomogeneities, which preserves the efficiency and intuitive qualities of the ray theory but is free from spurious environmental sensitivity and strong perturbations associated with ray trajectories.

- To investigate and quantify effects on underwater acoustic wavefronts of internal gravity waves, sea swell, "spice," and other small-scale processes in the water column.

OBJECTIVES

1. To assess significance of time dependence of the sound speed and flow velocity perturbations on predictability of acoustic wavefronts and timefronts.

2. To quantify horizontal refraction of sound by random meso-scale inhomogeneities at $O(1)$Mm propagation ranges.

3. To find the variance and bias of random ray travel times in the regime, where the ray displacement may be comparable to the vertical extent of the underwater waveguide but the clustering has not developed yet.

4. To determine, using a perturbation theory and numerical simulations, typical propagation ranges where clustering of chaotic rays replaces the anisotropy of ray scattering as the main physical mechanism responsible for acoustic wavefront stability.

5. To develop an efficient technique for modeling acoustic wavefronts and their perturbations in range-dependent and horizontally inhomogeneous oceans.

6. To model perturbations of acoustic wavefronts and timefronts by internal gravity waves, internal tides, sea swell, and "spice" in the ocean.

7. To investigate implications of wavefront stability on the downward extension of acoustic timefronts and deepening of lower turning points of steep rays due to small- and meso-scale physical processes in the upper ocean.

1. REPORT DATE **30 SEP 2013**	2. REPORT TYPE	3. DATES COVERED **00-00-2013 to 00-00-2013**
4. TITLE AND SUBTITLE **Dynamics and Stability of Acoustic Wavefronts in the Ocean**		5a. CONTRACT NUMBER
		5b. GRANT NUMBER
		5c. PROGRAM ELEMENT NUMBER
6. AUTHOR(S)		5d. PROJECT NUMBER
		5e. TASK NUMBER
		5f. WORK UNIT NUMBER
7. PERFORMING ORGANIZATION NAME(S) AND ADDRESS(ES) **CIRES/University of Colorado and NOAA/Earth System Research Lab,Physical Sciences Division, R/PSD99,325 Broadway,Boulder,CO,80305-3328**		8. PERFORMING ORGANIZATION REPORT NUMBER
9. SPONSORING/MONITORING AGENCY NAME(S) AND ADDRESS(ES)		10. SPONSOR/MONITOR'S ACRONYM(S)
		11. SPONSOR/MONITOR'S REPORT NUMBER(S)
12. DISTRIBUTION/AVAILABILITY STATEMENT **Approved for public release; distribution unlimited**		
13. SUPPLEMENTARY NOTES		
14. ABSTRACT		
15. SUBJECT TERMS		

16. SECURITY CLASSIFICATION OF:			17. LIMITATION OF ABSTRACT	18. NUMBER OF PAGES	19a. NAME OF RESPONSIBLE PERSON
a. REPORT **unclassified**	b. ABSTRACT **unclassified**	c. THIS PAGE **unclassified**	**Same as Report (SAR)**	**8**	

APPROACH

Our primary theoretical approach is an extension of the method employed in (Godin, 2003, 2007, 2009), where a novel perturbation technique has been developed to solve the eikonal equation and calculate wavefront and ray trajectory displacements, which are required to be small over a correlation length of the environmental inhomogeneities but not necessarily over the entire acoustic propagation path. Methods based on the geometrical acoustics are supplemented by full-wave approaches (Brekhovskikh and Godin, 1999), including a normal-mode theory for range-dependent and horizontally inhomogeneous waveguides.

The analytical methods are complemented by numerical wavefront-tracing techniques. A major problem with a direct modeling of acoustic wavefronts in the ocean through numerical solution of the eikonal equation lies in the eikonal (and acoustic travel time) being a multi-valued function of position. A number of computational approaches to solve the eikonal equation without ray tracing have been developed in mathematical and seismological communities (Vidale, 1990; Sava and Fomel, 2001; Sethian, 2001, Benamou, 2003). However, most of these methods are only capable of tracing the wavefront of the earliest, first arrival and thus are not suitable for underwater acoustic applications. We adapt to ocean acoustics problems the Lagrangian wavefront construction techniques (Vinje et al., 1993, 1999; Lambaré et al., 1996; Sava and Fomel, 2001; Chambers and Kendall, 2008; Hauser et al., 2008), which have been developed in the context of exploration seismology and are capable of computing all arrivals. Extension of the existing wavefront construction techniques to long-range underwater sound propagation is a non-trivial and, in fact, rather challenging task because the number of ray arrivals and topological complexity of wavefronts in the ocean far exceed those in the geophysical applications considered to date.

Theoretical results and new modeling capabilities are being verified against numerical simulations performed with well-established ray and PE propagation codes.

The key individuals that have been involved in this work are Oleg A. Godin (CIRES/Univ. of Colorado and NOAA/ESRL), Nikolay A. Zabotin (CIRES/Univ. of Colorado), and L. Y. Zabotina (ECEE/Univ. of Colorado). Dr. Zabotin and Ms. Zabotina focused on developing and testing an efficient computer code for modeling acoustic wavefronts in inhomogeneous, moving fluids. Dr. Godin took the lead in theoretical description of effects of the ocean currents, localized inhomogeneities, and sound-speed time-dependence on the acoustic wavefronts.

WORK COMPLETED

Effects of localized, strong gradients of environmental parameters on acoustic wavefronts have been investigated in idealized settings, which admit finite-frequency asymptotic solutions of the wave equation. Homogeneous and radially inhomogeneous fluid, solid, and fluid-solid scatterers have been considered (Godin, 2013a, b). The asymptotic solutions have been verified against finite-element numerical solutions (Glushkov et al., 2013).

The feasibility of using hydrophone arrays of unknown shape to retrieve regular, predictable wavefronts from wave fields scattered by the ocean surface and seafloor or generated by multiple incoherent sound sources has been demonstrated in numerical experiments (Goncharov et al., 2013).

It has been established that wavefront-tracing partial differential equations obtained from the Huygens' principle, from the eikonal equation, or from the differential ray equations are consistent. A broad class of finite-difference schemes has been derived to trace wavefronts. In anisotropic media and, in particular, in moving fluids one can choose to propagate wavefronts along rays, wave normals, or other auxiliary paths (Zabotin et al., 2013).

An exact analytic solution of the eikonal equation for a point source in a three-dimensionally inhomogeneous fluid has been obtained and applied to benchmark our 3-D wavefront tracing code (Godin and Zabotin, 2013).

Effects of random internal gravity waves with the Garrett-Munk spectrum on 3-D sound propagation have been quantified (Godin and Zabotin, 2013).

Evolution in time of acoustic wavefronts at 3-D sound propagation through a moving packet of nonlinear internal gravity waves in shallow water has been investigated (Zabotin et al., 2013).

RESULTS

A software package has been developed for numerical modeling of 3-D sound propagation in the ocean, where sound speed and current velocity are arbitrary smooth functions of three spatial coordinates. The package has been made freely available through the Ocean Acoustics Library, http://oalib.hlsresearch.com/. The software package is a numerical implementation of an alternative formulation of the geometrical acoustics, where wavefronts rather than rays are the geometric "backbone" of the wave field. Wavefront tracing can be viewed as a direct implementation of the Huygens' principle. Our current wavefront tracing algorithm (Zabotin et al., 2013) is an extension to three-dimensionally inhomogeneous, moving media of an earlier 2-D algorithm for sound in moving fluids (Zabotin et al., 2012) and the original Huygens Wavefront Tracing (HWT) algorithm (Sava and Fomel, 2001), developed as a part of the open-source Madagascar project for seismic modeling and imaging. Aside from generalization to moving media, the extended HWT algorithm improves the accuracy and stability of the original algorithm and includes new functionality to account for sound reflections at sloping boundaries and to efficiently model acoustic timefronts in addition to the wavefronts. For wavefront tracing in inhomogeneous media, HWT is much more computationally efficient and robust than traditional ray codes (Sava and Fomel, 2001). Unlike many other eikonal solvers, the HWT method produces the output in ray coordinates and has the important ability to track multiple arrivals. With the HWT method, each wavefront is generated from the preceding one by finite differences in the ray-coordinates domain.

The extended HWT algorithm has been benchmarked using exact analytic solutions of the eikonal equation for wavefronts due to a point source in various inhomogeneous and moving media (Zabotin et al., 2013), including the exact solution we obtained for the so-called Maxwell's "fish-eye" lens (Born and Wolf, 2002). In acoustic terms, Maxwell's "fish-eye" lens is an unbounded fluid with quadratic dependence $c = \left(1 + R^2/a^2\right)c_0$ of the sound speed c on distance R from the origin of coordinates. Here a and c_0 are positive constants. Rays in the "fish-eye" lens are arcs of circles; all rays leaving the point $\mathbf{R}_0$ gather at the point $\mathbf{R}_1 = -a^2R_0^2\,\mathbf{R}_0$ and form a perfect focus. After gathering at $\mathbf{R}_1$, rays first diverge and then again converge and form a perfect focus at $\mathbf{R}_0$, and the process repeats periodically with period $T = \pi a/c_0$. Wavefronts due to a point source are spheres in the Maxwell's "fish-eye" lens. At the

initial moment $t = 0$, the center of the sphere coincides with the sound source. As time t increases, the center moves along the straight line connecting $\mathbf{R}_0$ with the center of symmetry of the medium, goes to infinity, and the sign of curvature of the wavefront changes. At $t = 0.5\ T$, the wavefront collapses into the point $\mathbf{R} = \mathbf{R}_1$. Then the radius of the spherical wavefront increases again, its center moves away from $\mathbf{R}_1$, goes to infinity, and starts moving towards $\mathbf{R}_0$. At $t = T$, the wavefront collapses into the point $\mathbf{R} = \mathbf{R}_0$ and returns to its initial position at $t = 0$.

Repeated, perfect focusing of waves in the Maxwell's "fish-eye" lens presents a particularly stringent test of accuracy of numerical simulations of sound propagation. A comparison between the numerical results obtained using the 3-D HWT algorithm and the analytical solution is shown in Figure 1. The wavefront tracing algorithm accurately reproduces expansion of spherical wavefronts from the point source, their subsequent collapse into a perfect focus, and the next phase of expansion from the focus followed by collapse into the original sound source.

The 3-D HWT algorithm has been applied to study effects of various oceanographic processes on underwater sound propagation and also has been demonstrated to be an efficient and robust technique for modeling infrasound propagation in the atmosphere (Zabotin et al., 2013).
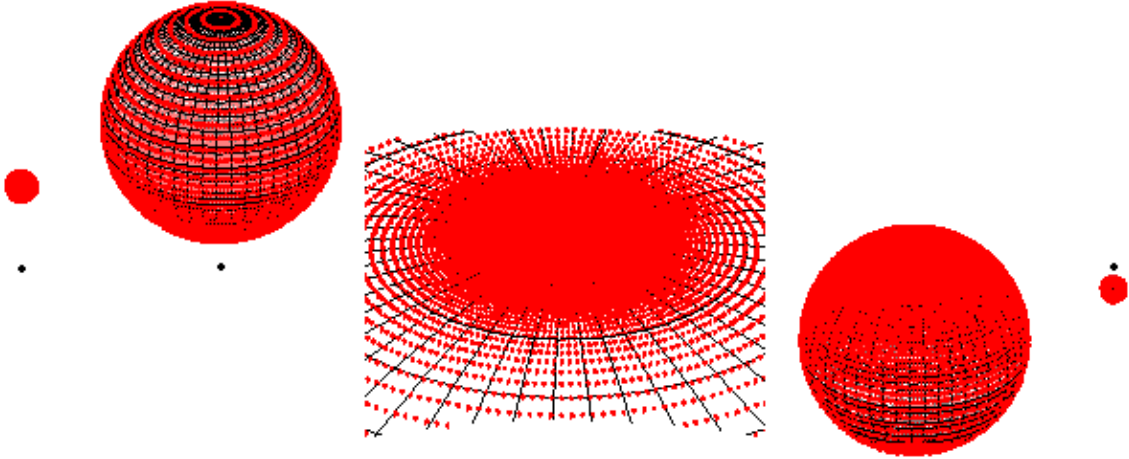

Figure 1. Time evolution of wavefronts in a 3-D benchmark problem known as Maxwell's "fish-eye" lens. A numerical solution for wavefronts obtained with the 3-D HWT algorithm (red dots) is shown superimposed on the analytical solution (black lines) of the problem. The center of symmetry of the medium is marked with the black dot. The two parameters of the lens are a = 5 km, c_0 = 1.5 km/s; the source shift from the center of symmetry is 10 km. The period of the transient wave field pulsations is T = 10.472 s. The five panels in the figure correspond to five consecutive steps in the wavefront evolution, covering approximately half of the period: t/T = 0.02, 0.1, 0.15, 0.21, 0.44 (from left to right).
[The wavefronts are spheres, with the wavefront at t/T = 0.15 having the largest radius of the five spheres shown. The centers of the spherical wavefronts are located above or below the center of symmetry of the medium at t/T = 0.02, 0.1 and t/T = 0.15, 0.21, 0.44, respectively.]

To illustrate application of the 3-D wavefront tracing to modeling sound propagation in shallow water, we consider environmental conditions similar to that of the 1995 Shallow-Water Acoustic Random Media (SWARM) experiment (Apel et al., 1997). Rather strong sound speed variations in time and in the horizontal plane were encountered during the SWARM experiment. The sound-speed variability was primarily due to packets of nonlinear internal gravity waves (IWs), which were generated by tides on a shelfbreak. We follow (Apel, 2003; Godin et al., 2006) and use the "dnoidal" model of the vertical isopycnal displacement in the nonlinear IW packets (Figure 2). In our simulations we placed the source of sound at the point with coordinates $x = 0$, $y = 5000$ m, $z = 20$ m, i.e., at the depth corresponding to the peak of the first IW mode shape function, and considered different positions of the center of curvature of the IW fronts. Figure 2 illustrates distortion of acoustic wavefronts by the IW packet at a time when the peak of the sound-speed perturbation reaches the vertical plane $y = 5000$ m. Evidence of horizontal refraction of sound can be seen in the upper panel of Figure 2. IW-induced multi-pathing and apparent "broadening" of timefronts are evident in the lower panel.
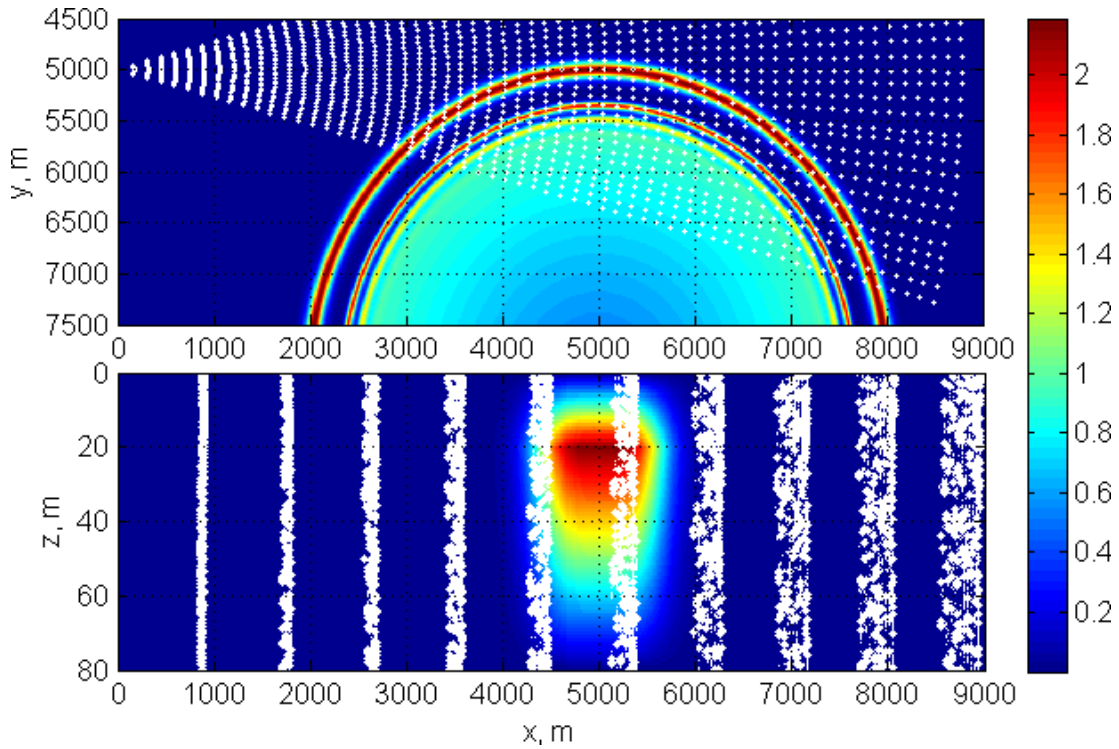

Figure 2. Underwater acoustic wavefronts at propagation through a train of nonlinear internal gravity waves. Projections of the wavefronts are shown on the horizontal plane z = 20 m (upper panel) and on the vertical plane y = 5000 m (lower panel) passing through the sound source located at the point (0, 5000 m, 20 m). The internal wave train originates at a location with horizontal coordinates x = 5000 m, y = 8000 m. The color scale shows the magnitude of the internal wave-induced displacement (in m) of an isopycnal surface from its unperturbed depth z = 20 m. White dots show projections of end points of rays, the original distribution of which on the wavefront was uniform, at ten consecutive times after sound emission by the source.
[The isopycnal displacement varies between zero and 2.1 m, is rotationally symmetric in the horizontal plane with respect to the point of the internal gravity wave train origin, and reaches its maximum at z = 20 m. Acoustic wavefronts are represented by strips in the vertical plane, which are parallel to the Oz coordinate axis and become progressively wider as the distance from the source increases from zero to 9000 m.]

Results of wavefront tracing can be used to determine a number of characteristics of the acoustic field. For some applications, prediction of bearing (i.e., azimuthal) and grazing angles of acoustic arrivals at the receiver are of primary interest. Figure 3 illustrates the effect of the IW packet on the bearing and grazing angles. We have calculated the direction of the wave normal at different points on a particular wavefront for various stages of the IW packet evolution and presented the results as histograms of the bearing and grazing angles perturbations relative to their values in the absence of IWs. As expected, perturbations in the sound propagation direction become stronger, on average, when acoustic rays penetrate deeper into the IW packet (Figure 3). The width of the distribution for the grazing angle is an order of magnitude larger than of its counterpart for the bearing angle. This is consistent with earlier results (Godin et al., 2006), which were obtained by a combination of 2-D ray tracing in the vertical plane and a perturbation treatment (Godin, 2002) of the horizontal refraction.
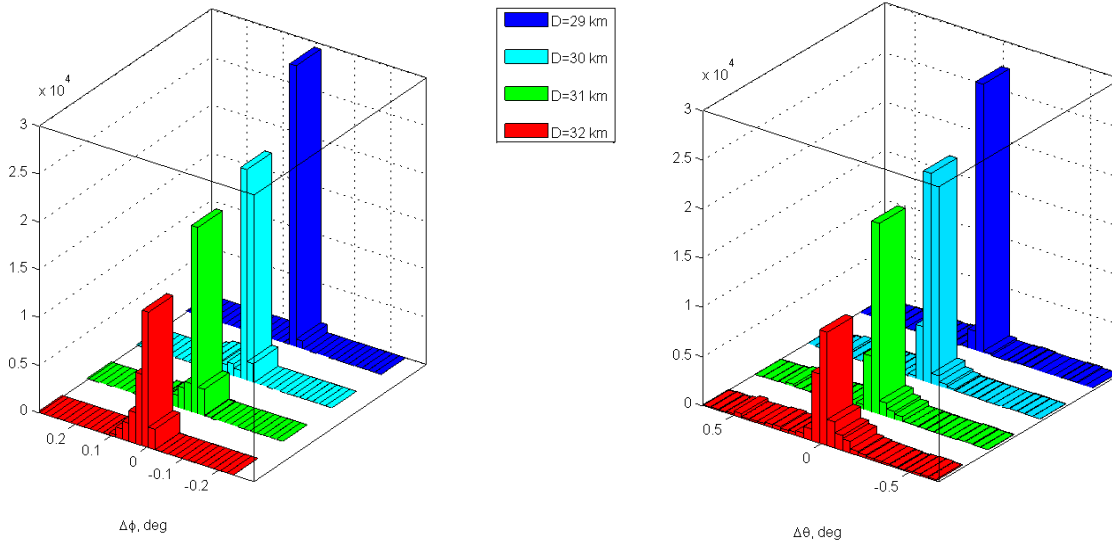

Figure 3. Internal wave-induced variations in the direction of sound propagation. Histograms of perturbations (in degrees) in bearing (left panel) and grazing angles (right panel) after 6 s of sound propagation from a point source are shown for four different stages of the nonlinear internal wave packet evolution. Perturbations in the direction of the wave normal are calculated for a section of the acoustic wavefront, which corresponds to azimuthal angles from –5° to 5° and grazing angles from –15° to 15° at the sound source. The internal wave train originates at a location with horizontal coordinates x = 5 km, y = 35 km. The packet occupies a circle with radius D = 29 km, 30 km, 31 km, or 32 km. When D = 30 km, the maximum of the sound speed perturbations reaches the y = 5 km plane.
[Four histograms are shown for each of the bearing and grazing angles at D = 29, 30, 31, and 32 km. Bearing and grazing angle perturbations are shown from –0.2° to 0.2° and from –0.5° to 0.5°, respectively. The histograms become wider and progressively less symmetrical with respect to zero as the parameter D increases.]

IMPACT/APPLICATIONS

Wavefront tracing has been established as a new approach to modeling sound fields in deep and shallow water, which readily accounts for 3-D propagation effects and current-induced acoustic anisotropy. In addition to modeling acoustic manifestations of internal gravity waves, internal tides, and swell in the ocean, wavefront tracing provides an efficient technique for simulating long-range propagation of infrasound and acoustic-gravity waves in the atmosphere.

RELATED PROJECTS

None.

REFERENCES

J. R. Apel, A new analytical model for internal solitons in the ocean, *J. Phys. Oceanogr.*, **33,** 2247–2269 (2003)

J. R. Apel, M. Badiey, C.-S. Chiu, S. Finette, R. Headrick, J. Kemp, J. Lynch, A. Newhall, M. Orr, B. H. Pasewark, D. Tielbuerger, A. Turgutt, K. von der Heydt, and S. Wolf, An overview of the 1995 SWARM shallow-water internal wave acoustic scattering experiment, *IEEE J. Ocean. Eng.*, **22**, 465–500 (1997)

J. D. Benamou, An introduction to Eulerian geometrical optics (1992-2002), *J. Sci. Computing*, **19**, 63-93 (2003)

M. Born and E. Wolf, *Principles of optics: electromagnetic theory of propagation, interference and diffraction of light*, 7th edn. (Cambridge Univ. Press, Cambridge, 2002)

L. M. Brekhovskikh and O. A. Godin, *Acoustics of Layered Media. 2: Point Sources and Bounded Beams*. 2nd edn. (Springer, Berlin etc., 1999)

K. Chambers and J.-M. Kendall, A practical implementation of wave front construction for 3-D isotropic media, *Geophys. J. Int.*, **174**, 1030–1038 (2008)

O. A. Godin, A 2-D description of sound propagation in a horizontally-inhomogeneous ocean, *J. Comput. Acoust.*, **10**, 123–151 (2002)

O. A. Godin, Systematic distortions of signal propagation times in random inhomogeneous media, *Doklady Physics*, **48**, 389–394 (2003)

O. A. Godin, Restless rays, steady wavefronts, *J. Acoust. Soc. Am.*, **122**, 3353–3363 (2007)

O. A. Godin, Stability of acoustic wave fronts propagating in anisotropic three-dimensional environments, *Acta Acustica united with Acustica*, **95**, 963–974 (2009)

O. A. Godin, V. U. Zavorotny, A. G. Voronovich, and V. V. Goncharov, Refraction of sound in a horizontally-inhomogeneous, time-dependent ocean, *IEEE J. Oceanic Eng.*, **31**, 384–401 (2006)

J. Hauser, M. Sambridge, and N. Rawlinson, Multiarrival wavefront tracking and its applications, *Geochem. Geophys. Geosyst.*, **9**, doi:10.1029/2008GC002069 (2008)

G. Lambaré, P. S. Lucio, and A. Hanyga, Two-dimensional multivalued traveltime and amplitude maps by uniform sampling of a ray field, *Geophys. J. Int.*, **125**, 584–598 (1996)

P. Sava and S. Fomel, 3-D traveltime computation using Huygens wavefront tracing, *Geophysics*, **66**, 883–889 (2001)

J. A. Sethian, Evolution, implementation, and application of level set and fast marching methods for advancing fronts, *J. Comput. Phys.*, **169**, 503-555 (2001)

J. E. Vidale, Finite-difference calculation of traveltimes in three dimensions, *Geophysics*, **55**, 521–526 (1990)

V. Vinje, K. Åstebøl, E. Iversen, and H. Gjøystdal, 3-D ray modeling by wavefront construction in open models, *Geophysics*, **64**, 1912–1919 (1999)

V. Vinje, E. Iversen, and H. Gjøystdal, Traveltime and amplitude estimation using wavefront construction, *Geophysics*, **58**, 1157–1166 (1993)

N. A. Zabotin, O. A. Godin, P. C. Sava, and L. Y. Zabotina, Acoustic wavefront tracing in inhomogeneous, moving media, *J. Comput. Acoust.*, **20**, Art, 125009 (2012).

PUBLICATIONS

E. V. Glushkov, N. V. Glushkova, and O. A. Godin, Effect of anomalous transparency of the water-air interface for a spherical sound source, *Acoust. Phys.*, **59**, 6–15 (2013) [published, refereed]

O. A. Godin, Rayleigh scattering of a spherical sound wave, *J. Acoust. Soc. Am.*, **133**, 709–720 (2013a) [published, refereed]

O. A. Godin, Rayleigh scattering of sound by spherically symmetric bodies, *Proc. Meetings Acoust.*, **19**, Art. 070009 (2013b) [published]

O. A. Godin and N. A. Zabotin, 3-D acoustic wavefront tracing in inhomogeneous, moving media. In: *Proc. 20th Int'l Congr. Sound and Vibr. (Bangkok, Thailand, 7–11 July 2013)*, Art. 81, pp. 1–8 (2013) [published]

V. V. Goncharov, Yu. A. Chepurin, and O. A. Godin, Passive acoustic tomography of the ocean using arrays of unknown shape, *Acoust. Phys.*, **59**, 170–178 (2013) [published, refereed]

N. A. Zabotin, O. A. Godin, P. C. Sava, and L. Y. Zabotina, Tracing three-dimensional acoustic wavefronts in inhomogeneous, moving media, *J. Comput. Acoust.* (2013)